A LINAC-TO-BOOSTER INJECTION LINE FOR TRANSVERSE MATCHING AND CORRELATED INJECTION PAINTING*

R. W. Garnett, L. J. Rybarcyk, LANL, Los Alamos, USA

Abstract

In this paper we discuss a compact linac-to-booster ring transfer line originally proposed for the Los Alamos Advanced Hydrotest Facility design to vertically inject a 157-MeV H^- beam from the linac into a 4-GeV booster. TRACE 3-D and PARMILA simulations were used to demonstrate the performance of the transfer line to deliver the required transverse beam to the foil while also allowing correlated longitudinal injection painting. Schemes for both transverse and longitudinal matching are important for high-intensity ring applications where low beam loss operation is desirable. The main features of the beam line layout, a proposed longitudinal painting scheme, and the simulation results will be discussed. This work is supported by the U. S. Department of Energy Contract W-7405-ENG-36.

INTRODUCTION

The most recent design of the Advanced Hydrotest Facility (AHF) assumes an injector linac that is a duplication of the SNS linac up to 157 MeV [1]. The linac is followed by an injection line that allows both transverse matching and correlated longitudinal injection painting [2,3] into a 4-GeV booster ring, followed finally by a 50-GeV main ring and associated beam lines for radiography. Here we propose a layout of an injection line that includes the required horizontal and vertical bends necessary to deliver the desired beam to the booster injection foil. Preliminary beam parameters required at the foil, which constrain the proposed transfer line design, and information regarding the booster lattice geometry were provided by the booster designers [4]. TRACE 3-D, PARMILA, and ESME2K simulations were used to demonstrate the performance of the transfer line to deliver the required transverse beam to the foil while also allowing longitudinal injection painting.

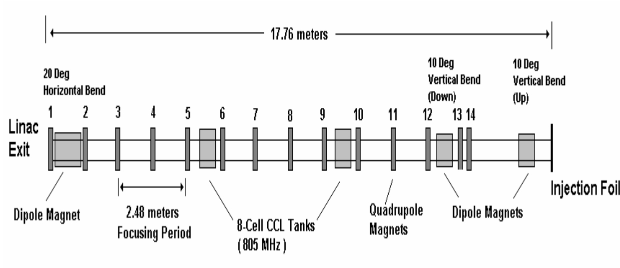

Figure 1: Unfolded layout of the booster transfer line.

TRANSFER LINE LAYOUT

Figure 1 shows the unfolded layout of the transfer line, including its various components. The layout of the transfer line relative to the booster ring is not shown, however, its length constrains the horizontal bend required with respect to the linac beam axis. The horizontal bend angle was chosen to allow sufficient separation between a separate linac tune-up line and the booster transfer line. A 20°-bend angle gives a sufficient separation to allow space for the required shielding so that linac tune-up activities can be in progress while maintenance activities, etc. are performed in the adjacent booster tunnel.

The transfer line focusing lattice is an extension of that used in linac. It was found that doing so maintains the beam size required to clear the relatively small radial apertures (r=1.5cm) of the 805-MHz 8-cell coupled-cavity linac (CCL) tanks of the transfer line that are used to do the correlated painting.

These cavities are identical to those of the last tank of the SNS CCL in order to save construction costs. The first tank will be operated in the bunching mode (ϕ= -90°). The second tank will be varied in phase about -90° and over a range sufficient to give the desired energy variation required to do the painting (typically -120°$\leq \phi \leq$ -60º). The amplitude settings of the tanks are not identical, but are well within the expected operating range for SNS.

The quads in the transfer line are all set to identical gradient values with the exception of the final 4 quads (11-14 as shown in Fig. 1) that are used to obtain the transverse beam parameters required at the injection foil. From simulation results it was found that the dispersion at the foil could be reduced significantly by operating the last part of the linac and the transfer line at nearly 90° transverse zero-current phase advance. This results in somewhat higher quadrupole gradients as previously specified for SNS, but well within their operational limits.

Table 1 gives some of the transfer line mechanical and operational parameters. The total unfolded length of the transfer line from the linac exit to the foil is 17.8m. The magnetic field for all three bending dipoles is limited to 0.75 Tesla to avoid magnetic stripping of the H^- beam [5].

BOOSTER INJECTION REQUIREMENTS

Figure 2 shows the vertical injection region into the booster. It has been assumed that all magnets in this region will be operating in DC-mode. The long straight section in the booster is approximately 8.4m long. The injection region is assumed to occupy approximately 7m of the straight section as is shown in the figure. The combination of dipoles in the injection region will bend the beam upward by 10° and then back to horizontal at a new elevation. This displaces the beam approximately 0.53m off the booster axis during injection. This particular geometry requires the linac beam centerline to be approximately 1.3m above the ring axis with a gradual change in elevation to the ring axis after the downward 10°-bend in the transfer line. A vertical clearance of approximately 0.9m between the booster magnets and the elements in the transfer line where the two lines tangentially and vertically merge.

Table 1. Transfer line parameters.

Transverse Focusing Lattice	Quadrupole Singlet
Transverse Focusing Period	2.48 m
Zero-Current Transverse Phase Advance / Period	≈ 90 degrees
Quadrupole Effective Length	8 cm
Focusing Quads	26.67 T/m
Matching Quads Q11, Q12, Q13, Q14	-37.97 T/m, 17.40 T/m, -41.28 T/m, -41.28 T/m
8-Cell CCL Tank Length	76.62 cm
Tank 1 Accel Gradient (EoT)	1.80 MV/m
Tank 2 Accel Gradient (EoT)	2.30 MV/m
CCL Bore Radius	1.5 cm
Dipole Magnetic Field, B	0.75 Tesla
Dipole Radius of Curvature, ρ	2.52 m

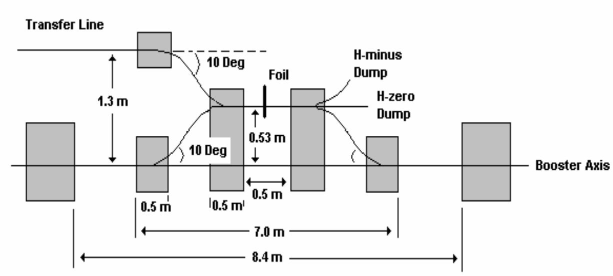

Figure 2: Booster injection region geometry. The final four transfer line quads were adjusted to meet the beam requirements at the foil.

TRANSFER LINE SIMULATIONS RESULTS

The TRACE 3-D beam envelope code was used initially to determine the transfer line layout. The location of the first CCL tank was selected by observing how rapidly the beam de-bunches as it exits the linac. The first tank was placed at a location where the total phase width of the beam is less than approximately 20°. This was specifically done to reduce the nonlinear effects on the beam distribution by the tank RF fields. The position of the second tank is chosen to minimize both the phase width and energy width at the foil. This solution leads to minimum variations in the longitudinal phase space of the beam as the second tank phase is varied to shift the beam energy centroid. Based on these simulation results, the expected x- and y-dispersion values are -0.348 m/frac and -0.035 m/frac, respectively; well within the requirements.

Multi-particle simulations using the PARMILA code were used to verify the beam envelope calculations. Design input files describing the SNS linac were obtained from the SNS project along with input beam distributions that are believed to be representative of the experimentally measured RFQ output. Simulations were completed using this input beam distribution to obtain the input distribution at the entrance to the transfer line. Table 2 gives the linac output beam parameters at the injection foil as calculated by PARMILA as a function of the CCL tank 2 phase settings. We have met the requirements specified above with our layout and choice of operational parameters. Figure 3 shows simulation results for the three nominal CCL-tank-2 phase settings of -60°, -90°, and -120°. The longitudinal phase space plots are shown.

CORRELATED PHASE-ENERGY PAINTING

The chopper in the low-energy beam transport of the linac. Along with the two CCL tanks of the transfer line, will be used to structure the train of micropulses in time. As described earlier, the second CCL tank will be used to change the central energy of the beam micropulses over the duration of a macropulse. By synchronizing the chopper and the energy-slewing cavity, a correlated longitudinal distribution can be produced. A simplified diagram of this system is shown in Figure 4. In this scheme, a gate signal will be simultaneously sent to the chopper and to a ramp generator which feeds a phase shifter on the low-level RF (LLRF) drive for the generator powering the CCL tank. The gate signal will enable a pre-programmed chopper pattern to begin. The LLRF drive signal will be modulated with a linear phase ramp which shifts the phase of the RF, as seen by the beam, by 100° over the macropulse. This will result in an almost linear variation of the beam energy across the macropulse. A negligible 10.5-kHz detuning of the 805-MHz tank is expected during the required phase variation of the cavity for a 25-turn injection (26.4 μs) into the booster. The field amplitude in the tank will operate at approximately 62% of the nominal design value (2.1 MV/m vs. 3.37 MV/m).

The goal of employing this scheme is to inject a matched beam into the booster RF bucket to minimize losses. The separatrix of a stationary RF bucket made up of RF harmonic h=1 has the shape of $\pm\Delta W\cdot\mathrm{Cos}(\phi/2)$ where $-180° \le \phi \le 180°$ and ΔW is the maximum energy extent of the bucket relative to the nominal injection energy of the booster. The energy of the injected beam will be swept in a monotonic fashion from $-\Delta W$ to $+\Delta W$ over the duration of the macropulse. During each "turn" of injected beam in the booster, the phase duration of that train of micropulses will be truncated by the beam chopper to match it to the phase width of the RF bucket

Table 2: Output beam parameters at the foil as calculated from the PARMILA simulations.

Tank 2 Phase	α_x	α_y	β_x (mm/mrad)	β_y (mm/mrad)	ε_x (π-cm-mrad, norm)	ε_y (π-cm-mrad, norm)	Beam Energy
-60°	-0.006	-0.058	9.98	9.61	0.0329	0.0519	157.91
-90°	0.023	-0.062	10.02	9.57	0.0331	0.0524	157.04
-120°	0.089	-0.047	9.68	9.37	0.0331	0.0520	156.19

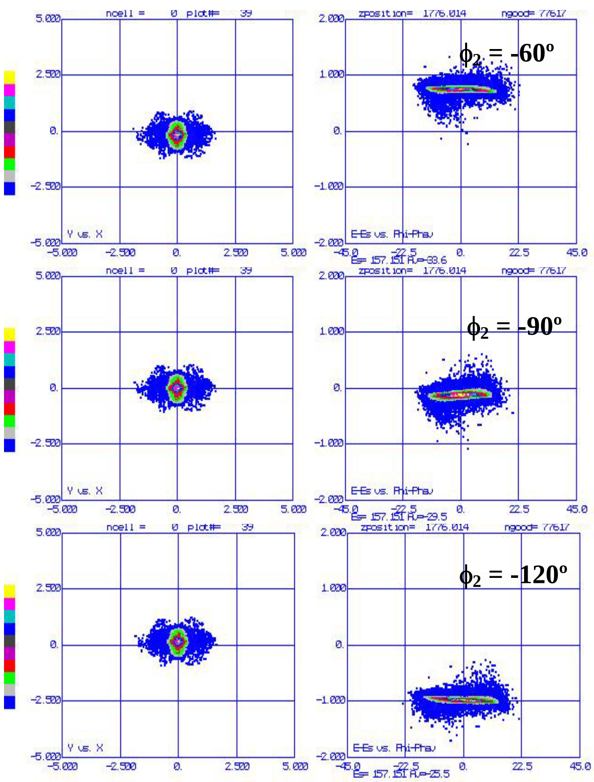

Figure 3: PARMILA simulation results: xy-beam spot at the foil and the longitudinal phase space distribution for the three CCL tank 2 phase settings.

for that energy offset. Figure 5 shows the longitudinal phase space distribution in the booster at the end of the 25-turn injection for a beam created in this fashion and simulated using ESME2K**.** To create this matched beam, three output distributions from PARMILA simulations described earlier were used, i.e. for tank 2 phase = -90° and ±50° from the nominal (-40° and -140°). These distributions were analyzed to determine the average energy and energy width of each distribution. This information was used along with a simple representation of the second CCL tank RF field, i.e. $V \cdot \sin \phi$, to produce the energy variation versus turn needed to paint into the RF bucket. The number of particles injected during each turn was adjusted by the amount of chopping done to the beam. A constant peak current from the linac was assumed. The beam was chopped to a maximum phase extent of ±170° to better match the pseudo-stationary RF bucket. To achieve the required 5×10^{12} protons injected into the booster (156m circumference) over the 25 turns (in 26.4 μs), at a nominal injection energy of 140 MeV, an average current of ~30.3 mA over the macropulse will be required. This is equivalent to a 50.3-mA-peak-beam current during the macropulse..

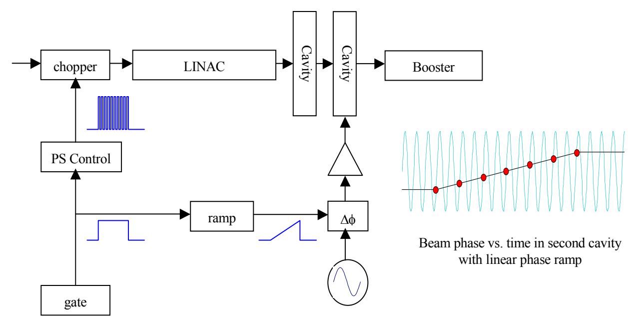

Figure 4: Schematic of the correlated longitudinal painting system. The drive signal to the sweeping cavity is phase modulated with a linearly-increasing phase to sweep the beam across the desired range of phase over the macropulse. The modulation is synchronized with the chopping pattern and the booster RF.

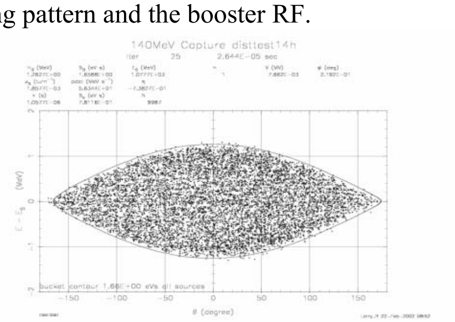

Figure 5: ESME2K simulation results showing the matched beam distribution injected into the booster over 25 turns. The second CCL tank provided ~1.15 MeV of energy variation over a range of 50° of phase as seen by the linac beam.

REFERENCES

[1] AHF Quarterly Report, April 25, 2002.

[2] R. Garnett and L. Rybarcyk, "AHF Linac Simulations Including Correlated Painting," Los Alamos National Laboratory Technical Memorandum, LANSCE-1:02-015, February 26, 2002

[3] L. Rybarcyk, "ESME Simulation Results for Matched Beam Injection into AHF Booster with Resonant Magnet Power Supplies", Los Alamos National Laboratory Technical Memorandum, LANSCE-1:02-012TN, February 26, 2002.

[4] F. Neri, private communication.

[5] A. Jason, D. Hudgings, and O. van Dyck, "Neutralization of H- Beams by Magnetic Stripping," IEEE Transactions on Nuclear Science, Vol. NS-28, No. 3, June 1981.